ACS OMEGA

http://pubs.acs.org/journal/acsodf

Article

Energy Calculation and Simulation of Methane Adsorbed by Coal with Different Metamorphic Grades

Xiangchun Li,* Xiaolong Chen,* Fan Zhang, Mengting Zhang, Qi Zhang, and Suye Jia

Cite This: *ACS Omega* 2020, 5, 14976−14989

Read Online

ACCESS | Metrics & More | Article Recommendations

ABSTRACT: The law of specific surface energy variation during the adsorption process is an important basis for studying the mechanisms of coal gas adsorption. Based on the theory of adsorption energy, eight coal samples with different ranks were analyzed using an isothermal adsorption experiment at three different temperatures (30, 40, and 50 °C) and six different pressures (0.1, 0.2, 0.6, 1.0, 1.4, and 1.8 MPa). Then, the single-layer adsorption model and multilayer adsorption model were used to calculate the energy variation during the adsorption process. Just like the adsorption capacity, it is clear that the specific surface energy is inversely proportional to temperature and proportional to gas pressure. The energy difference between the single-layer adsorption and the multilayer adsorption calculation is large. Therefore, the adsorption energy was calculated based on the calorific value, and the comparative analysis shows that the specific surface energy based on the multilayer adsorption model can better reflect the gas adsorption capacity than the single-layer adsorption model. The mechanisms of gas adsorption were explored, such as intermolecular force, energy variation, and specific surface area. The adsorption energy was simulated, which indicated that the energy variation is affected by both coal physical properties and internal chemical structure.

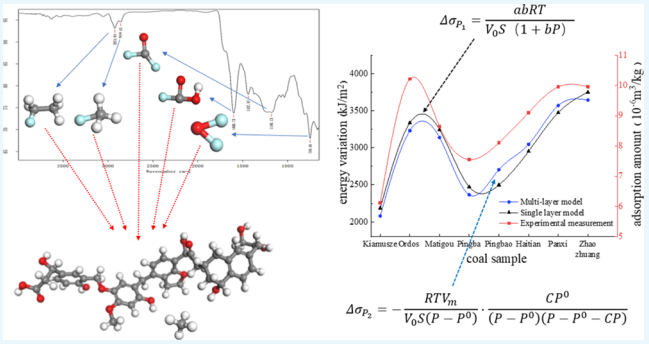

1. INTRODUCTION

Coal and gas outburst accidents have always been one of the important factors restricting the development of the mining industry.[1,2] In addition, because of the increased demand for energy, increasing coalbed methane (CBM) extraction efficiency is also urgently needed.[3] Therefore, understanding the gas adsorption mechanism and investigating the adsorption capacity are necessary. The adsorption capacity is not only impacted by the coal characteristics, such as pore structure[4,5] and molecular physicochemical structure, but also by the environment around coal seams, such as gas pressure and temperature.[6] The pore structures can provide a very large specific surface area for gas adsorption, and the size changes as the metamorphic degree increases.[7] The functional clusters on the coal surface affect the adsorption energies, which ultimately leads to differences in the gas adsorption capacity.[8] Both temperature and gas pressure affect the kinetic energy of gas molecules, and the adsorption capacity decreases with increasing temperature.[9] However, as the gas pressure increases, the probability of collision of gas molecules with the coal surface increases, which in turn improves the adsorption capacity.[10]

Based on a large number of experimental results, the adsorption kinetic models were addressed, such as the Langmuir single-layer adsorption theory,[11,12] Brunauer−Emmett−Teller (BET) multilayer adsorption theory,[13,14] and adsorption potential theory.[15] The Langmuir model and BET model seemed to be the two most practical models and the basis for many researchers to investigate the mechanisms of coal gas adsorption. The essence of adsorption is a spontaneous tendency of coal to reduce specific surface energy by reducing surface tension, and the mutual electric force between the coal surface and methane molecules causes the coal to adsorb a large amount of gas.[16] Consequently, the differences in the chemical and physical structures of coal molecules are the fundamental reasons for the significant differences in the adsorption−desorption of CBM.[17] The specific surface energy is a physical property and is the sum of the interaction forces between the interfaces.[18] Thus, it provides a means of investigating the adsorption mechanism. Zhou et al.[19] analyzed the surface energy variation and the equivalent adsorption heat based on the thermodynamic

Received: February 1, 2020
Accepted: June 1, 2020
Published: June 16, 2020

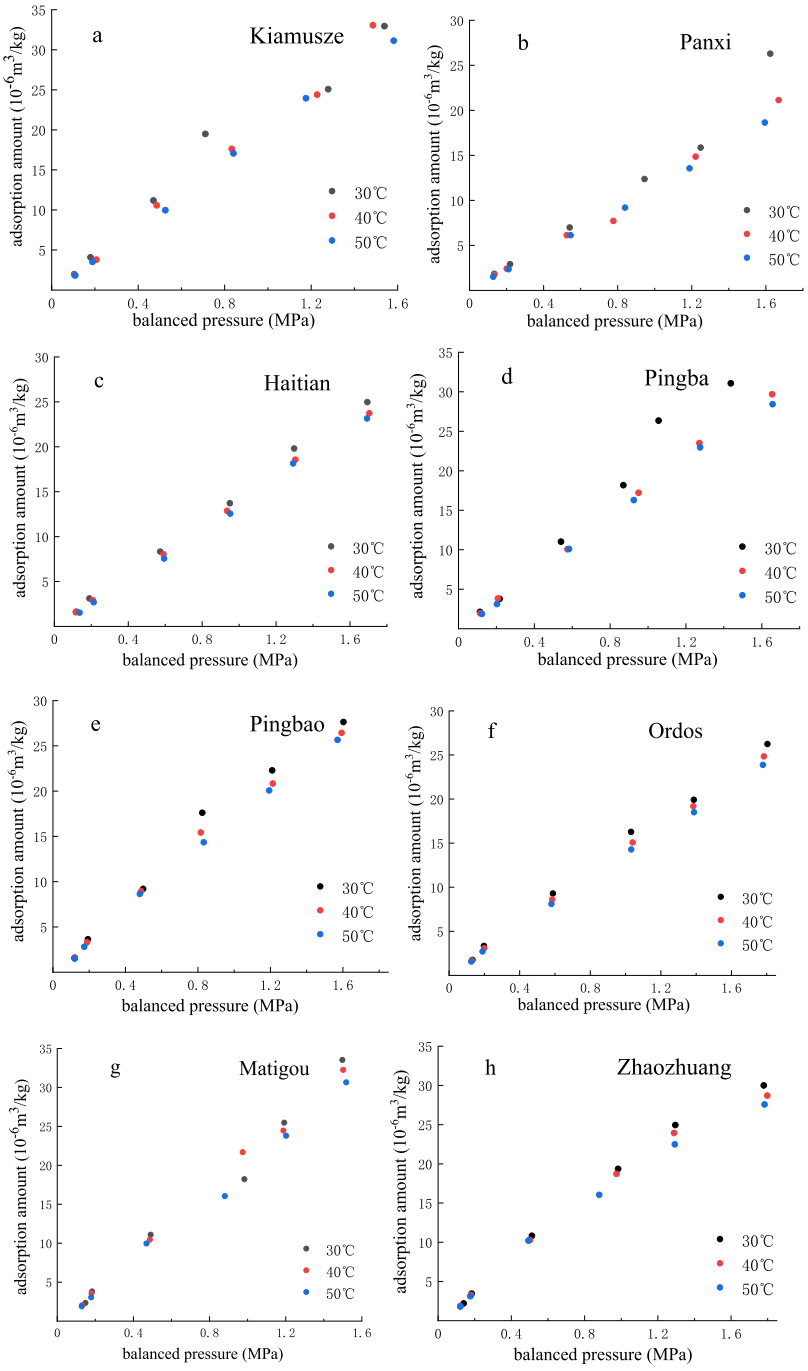

Figure 1. Isothermal adsorption curve of coal samples at 30 °C (black), 40 °C (red), and 50 °C (blue). Kiamuse (a); Panxi (b); Haitian (c); Pingba (d); Pingbao (e); Ordos (f); Matigou (g); Zhaozhuang (h).

theory and proposed that CO_2 and CH_4 will compete for adsorption during the adsorption process. The specific surface energy of coal contains not only apolar but also polar (electron donor) interfacial interactions,[20] and the polar components can be partially blocked by the specific surface energy component.[21] Burdzik et al.[22] obtained a reference value for specific surface energy by analyzing the polar supercritical fluid extraction components of different polymer samples. Zhang et al.[23] demonstrated that the gas adsorption volume, coal surface structure, temperature, and pressure determine the reduction of surface tension and the adsorption capacity stronger as the surface tension reduction.

In recent years, most researchers have conducted the isothermal adsorption experiments to investigate the adsorption mechanism based on the pore structure and interaction force, not specific surface energy. On the other hand, less published literature is available on the specific surface energy calculation model of adsorption. In this study, according to the isothermal adsorption experimental data, adsorption models and molecular simulations were combined to characterize the specific surface energy and the adsorption mechanism. Meanwhile, we proposed a specific surface energy calculation model based on a reasonable adsorption model to better describe the adsorption mechanism and verified it with the calorific value.[24,25]

https://dx.doi.org/10.1021/acsomega.0c00462
ACS Omega 2020, 5, 14976−14989

Table 1. Specific Surface Area

coal sample	Kiamusze	Panxi	Haitian	Pingba	Pingbao	Matigou	Ordos	Zhaozhuang
specific surface area (m^2/g)	64.72	83.48	79.13	110.34	114.78	85.90	65.22	149.41

Table 2. Parameter Fitting Result of the Langmuir Equation of the Coal Sample

	Kiamusze			Panxi			Haitian			Pingba		
T/°C	a	B	R^2	a	b	R^2	a	b	R^2	a	b	R^2
30	14.6843	2.1149	0.97	18.939	3.3000	0.98	17.9533	4.4560	0.99	25.0352	1.1859	0.99
40	13.1406	4.8471	0.99	17.8253	5.5000	0.99	17.0648	12.2083	0.99	23.1489	0.9489	0.99
50	11.8064	13.0308	0.99	16.6945	4.7920	0.99	14.8368	6.3585	0.99	21.8412	0.9056	0.99
	Pingbao			Matigou			Ordos			Zhaozhuang		
T/°C	a	b	R^2	a	b	R^2	a	b	R^2	a	b	R^2
30	26.0417	1.0026	0.99	19.4892	5.6348	0.99	14.7985	2.3590	0.99	33.8983	1.9156	0.99
40	25.5754	0.7476	0.99	18.3358	3.1595	0.99	13.5895	3.5842	0.99	33.0033	1.6648	0.99
50	21.0526	0.7208	0.99	17.0954	2.4849	0.98	12.5582.	3.9581	0.99	31.4465	1.4521	0.99

2. RESULTS AND DISCUSSION

2.1. Experimental Result. The adsorption amount is inversely proportional to temperature and proportional to pressure.[26−28] Figure 1 shows the isothermal adsorption capacity of eight different coal samples at 30, 40, and 50 °C. However, the data of the Kiamusze sample (a) at 30 °C and 1.4 MPa and the Pingba sample (d) at 30 °C and 1.4 MPa are atypical, and we believe the reason is that the gas pressure is not adjusted to the specific value (1.4 MPa) determined by the experimental scheme.

2.2. Specific Surface Energy Calculation. Gas is mainly adsorbed on the pore surface of the coal. During the isothermal adsorption process, the energy of the gas molecules will be released, and it can be reflected by the thermodynamic changes.[1] Adsorption is based on energy variation, and the absorption capacity can be characterized by the adsorption energy.

Coal is a macromolecular structure formed by different basic structural units connected by various bridge bonds. Moreover, the carbon atoms attract each other to reach equilibrium.[29] When the coal pores are formed, the carbon atoms on the surface are in an unbalanced state, resulting in the tendency that the atoms move toward the inside of the coal particle because of the intermolecular force. Meanwhile, the carbon atoms on the coal surface will obtain a specific surface energy.[30]

The carbon atoms in the surface layer of the coal pores always try to attract the surrounding gas molecules to reduce their specific surface energy and thus reach equilibrium.[31] Consequently, the methane concentration in the coal surface area must be higher than that which is in the coal matrix.[32] This difference is called the surface excess energy (Γ)

$$\Gamma = \frac{V}{V_0 S} \tag{1}$$

where Γ is the surface excess; V is the adsorption amount; V_0 is the molar volume; and S is the specific surface area of coal.

The surface tension will decrease during gas adsorption, and reduction can be calculated using eq 2

$$-\mathrm{d}\sigma = RT\Gamma \mathrm{d}(\ln P) \tag{2}$$

where σ is the surface tension after adsorption; R is the universal gas constant; T is the absolute temperature; and P is the gas pressure.

With eqs 1 and 2, integrating the gas pressure from 0 to P, the following can be written[33,34]

$$\Delta\sigma = \sigma_0 - \sigma = \frac{RT}{V_0 S}\int_0^P \frac{V}{P}\,\mathrm{d}P \tag{3}$$

where σ_0 is the surface tension under vacuum.

2.2.1. Single-Layer Adsorption. For single-layer adsorption, the specific surface energy variation ($\Delta\sigma_{P_1}$) at each pressure point can be defined as (see Appendix A)

$$\Delta\sigma_{P_1} = \frac{abRT}{V_0 S(1+bP)} \tag{4}$$

where a is the saturated adsorption capacity and b is the adsorption equilibrium constant.

According to the saturated adsorption capacity, the specific surface area of coal can be expressed as follows

$$S = aN_A\delta/V_0 \tag{5}$$

where S is the specific surface area; N_A is the Avogadro constant; and δ is the cross-sectional area of the gas molecules.

According to the adsorption data, the gas adsorption constants a and b under the isothermal condition can be tested based on the Langmuir equation. The cross-sectional area of the methane molecule is 16.4×10^{-20} m^2, and the gas adsorption specific surface area can be calculated using eq 5.[35] The results are shown in Table 1.

According to the isothermal adsorption experimental data, fitting the Langmuir adsorption equation can obtain the values of a and b of eight coal samples at different temperatures. The results are listed in Table 2.

For single-layer adsorption, the specific surface energy variation at different temperatures and pressures can be calculated using eq 4. The results are listed in Table 3.

2.2.2. Multilayer Adsorption. For multilayer adsorption, the specific surface energy variation ($\Delta\sigma_{P_2}$) can be defined as (see Appendix A)

$$\Delta\sigma_{P_2} = -\frac{RTV_m}{V_0 S(P-P_0)}\cdot\frac{CP_0}{(P-P_0)(P-P_0-CP)} \tag{6}$$

where V_m is the multilayer saturated adsorption capacity of coal; C is the constant related to sample adsorption capacity; and P_0 is the gas-saturated vapor pressure.

https://dx.doi.org/10.1021/acsomega.0c00462
ACS Omega 2020, 5, 14976−14989

Table 3. Specific Surface Energy Variation

	30 °C		40 °C		50 °C	
coal sample	equilibrium pressure (MPa)	change value (kJ/m^2)	equilibrium pressure (MPa)	change value (kJ/m^2)	equilibrium pressure (MPa)	change value (kJ/m^2)
Kiamusze	0.13	690.92	0.13	690.00	0.13	516.60
	0.23	1734.34	0.22	1571.82	0.24	1465.72
	0.59	2549.32	0.61	2248.41	0.64	2185.71
	1.02	3275.04	1.05	2847.28	1.01	2873.08
	1.40	3804.92	1.38	3373.77	1.38	3415.84
	1.78	4238.68	1.82	3770.28	1.83	3825.15
Panxi	0.11	1058.52	0.11	1179.00	0.11	890.55
	0.21	2621.91	0.22	2714.49	0.21	2346.62
	0.58	3822.81	0.58	3772.00	0.59	3474.91
	0.97	4738.54	0.98	4592.81	0.98	4409.82
	1.40	5359.26	1.38	5244.16	1.37	5097.77
	1.76	5858.19	1.79	5717.19	1.80	5580.89
Haitian	0.12	908.64	0.12	815.22	0.12	780.21
	0.22	2035.67	0.22	1975.61	0.20	1940.61
	0.61	3251.52	0.61	2987.00	0.63	2952.00
	1.01	4593.31	1.03	4290.31	1.01	4255.32
	1.38	4981.32	1.39	4529.01	1.40	4494.00
	1.78	5206.25	1.77	5033.32	1.76	4998.31
Pingba	0.12	429.48	0.12	336.11	0.14	301.11
	0.21	1556.49	0.22	1496.49	0.22	1461.53
	0.61	2772.41	0.62	2507.92	0.61	2472.88
	1.01	4114.17	0.98	3811.18	0.99	3776.19
	1.42	4502.19	1.39	4049.88	1.40	4014.91
	1.80	4727.14	1.79	4554.17	1.80	4519.22
Pingbao	0.13	455.37	0.12	362.00	0.12	327.00
	0.22	1582.38	0.21	1522.41	0.20	1487.43
	0.63	2798.31	0.61	2533.83	0.60	2498.77
	1.10	4140.10	1.08	3837.14	1.06	3802.08
	1.40	4528.12	1.39	4075.77	1.40	4040.82
	1.82	4753.22	1.80	4580.12	1.79	4545.15
Matigou	0.11	827.90	0.12	948.46	0.12	660.00
	0.19	2391.38	0.18	2484.00	0.17	2116.13
	0.49	3592.31	0.48	3541.44	0.47	3244.42
	0.82	4508.12	0.81	4362.29	0.83	4179.32
	1.20	5128.78	1.21	5013.67	1.19	4867.28
	1.60	5627.67	1.59	5486.72	1.57	5350.38
Ordos	0.13	920.54	0.12	1041.00	0.12	752.49
	0.18	2483.94	0.17	2576.52	0.17	2208.67
	0.51	3684.77	0.50	3634.00	0.49	3336.92
	0.98	4600.58	0.97	4454.83	0.88	4271.81
	1.29	5221.32	1.28	5106.18	1.29	4959.82
	1.77	5720.22	1.79	5579.17	1.78	5442.88
Zhaozhuang	0.14	1333.41	0.13	1453.89	0.12	1165.43
	0.18	2896.82	0.18	2989.43	0.17	2621.49
	0.49	4097.69	0.48	4046.93	0.46	3749.77
	0.98	5013.48	0.97	4867.71	0.88	4684.75
	1.19	5634.19	1.18	5519.12	1.20	5372.72
	1.49	6133.11	1.50	5992.09	1.51	5855.79

The specific surface area of coal can be calculated using eq 7[36]

$$S_{BET} = V_m A\sigma \quad (7)$$

where A is the cross-sectional area of gas molecules.

For multilayer adsorption, the specific surface energy variation at different temperatures and pressures can be calculated using eq 6. The results are listed in Table 4.

According to the experiment, the adsorption amount of coal samples increases as the pressure increases and the temperature decreases, which indicates that the gas adsorption is an exothermic process. Furthermore, under the same temperature condition, the relationship between the adsorption amounts of the eight coal samples is as follows: Zhaozhuang > Panxi > Ordos > Haitian > Matigou > Pingbao > Pingba > Kiamusze.

As shown in Figure 2, under the same temperature and pressure conditions, the specific surface energy variation and

https://dx.doi.org/10.1021/acsomega.0c00462
ACS Omega 2020, 5, 14976−14989

Table 4. Specific Surface Energy Variation

	30 °C		40 °C		50 °C	
coal sample	equilibrium pressure (MPa)	change value (kJ/m^2)	equilibrium pressure (MPa)	change value (kJ/m^2)	equilibrium pressure (MPa)	change value (kJ/m^2)
Kiamusze	0.13	585.10	0.13	584.20	0.13	410.80
	0.23	1628.52	0.23	1466.00	0.24	1359.91
	0.59	2443.47	0.61	2142.62	0.64	2079.92
	1.02	3580.92	1.05	3153.20	1.01	3179.00
	1.40	4110.77	1.38	3679.71	1.38	3721.72
	1.78	4544.56	1.82	4076.22	1.83	4131.00
Panxi	0.11	1364.44	0.11	1484.92	0.11	1196.42
	0.21	2516.11	0.22	2608.68	0.21	2240.77
	0.58	3717.00	0.58	3666.25	0.59	3369.12
	0.97	4632.79	0.98	4487.00	0.98	4304.00
	1.40	5665.22	1.38	5550.11	1.37	5403.73
	1.76	6164.09	1.79	6023.11	1.81	5886.77
Haitian	0.12	1214.52	0.12	1121.14	0.13	1086.12
	0.22	2341.47	0.23	2281.49	0.21	2246.51
	0.61	3145.69	0.61	2881.18	0.63	2846.21
	1.01	4487.48	1.03	4184.48	1.01	4149.49
	1.38	4875.49	1.392	4423.21	1.40	4388.22
	1.78	5100.41	1.77	4927.51	1.76	4892.47
Pingba	0.12	323.73	0.12	230.33	0.14	195.32
	0.21	1450.72	0.22	1390.72	0.22	1355.71
	0.61	2666.62	0.62	2402.10	0.61	2367.11
	1.01	4420.14	0.98	4117.12	0.99	4082.13
	1.42	4808.12	1.39	4355.79	1.40	4320.78
	1.80	5033.00	1.79	4860.10	1.80	4825.12
Pingbao	0.13	761.36	0.12	667.87	0.12	632.88
	0.22	1476.58	0.21	1416.63	0.20	1381.63
	0.63	3104.21	0.61	2839.72	0.60	2804.65
	1.10	4446.00	1.08	4143.00	1.06	4108.00
	1.40	4834.00	1.39	4381.67	1.40	4346.73
	1.82	5058.92	1.80	4886.00	1.79	4851.00
Matigou	0.12	722.21	0.12	842.69	0.12	554.23
	0.19	2285.58	0.18	2378.22	0.17	2010.29
	0.49	3486.49	0.48	3435.71	0.47	3138.58
	0.82	4814.00	0.81	4668.21	0.83	4485.22
	1.20	5434.73	1.21	5319.59	1.19	5173.21
	1.60	5933.58	1.59	5792.55	1.57	5656.31
Ordos	0.13	814.72	0.12	935.23	0.12	646.74
	0.18	2378.09	0.17	2470.70	0.17	2102.77
	0.51	3579.00	0.50	3528.20	0.49	3231.14
	0.98	4906.52	0.97	4760.70	0.88	4577.68
	1.29	5527.18	1.28	5412.11	1.29	5265.66
	1.77	6026.12	1.79	5885.13	1.78	5748.82
Zhaozhuang	0.14	1227.59	0.13	1348.15	0.12	1059.60
	0.18	2791.00	0.18	2883.62	0.17	2515.70
	0.49	3991.92	0.48	3941.11	0.46	3644.00
	0.98	5319.43	0.97	5173.64	0.88	4990.55
	1.19	5940.11	1.18	5825.00	1.20	5678.58
	1.49	6439.00	1.50	6298.00	1.51	6161.72

adsorption capacity have the same tendency as the coal rank increases. This means that the established specific surface energy calculation formula can accurately reflect the gas adsorption capacity, which verifies the reasonableness of the formula. The specific surface energy variation of the high-rank bituminous and anthracite coal samples is significantly higher than that of the low-rank bituminous coal, while the middle-rank bituminous coal samples are the lowest in the specific surface energy variation. The coal rank is the main factor controlling the gas adsorption capacity.[37−39] Micropores (<10 nm) are the main adsorption space for gas in coal. The percentage of the total pore volume occupied by the micropore volume increases as the coal rank increases; however, the micropore volume presents a trend of high−low−high variation because of the changes of the total pore volume.[7]

Comparing the results calculated using the two models, the difference is large. The single-layer adsorption model is based on the assumption that coal is an organic solid composed of

https://dx.doi.org/10.1021/acsomega.0c00462
ACS Omega 2020, 5, 14976−14989

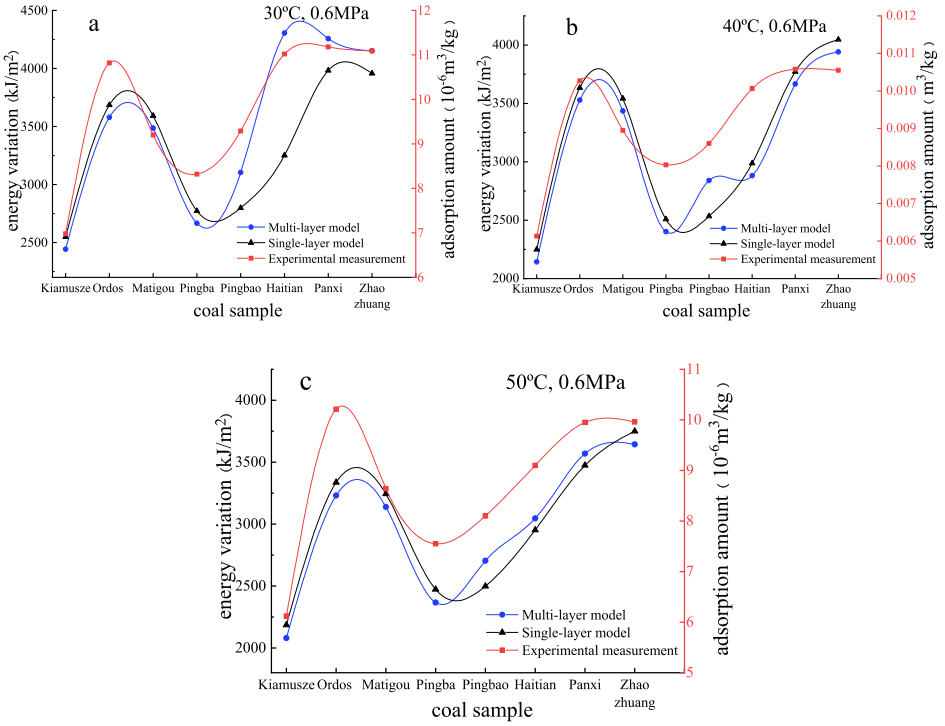

Figure 2. Adsorption amount and energy variation using different models at 30 °C, 0.6 MPa (a); 40 °C, 0.6 MPa (b); 50 °C, 0.6 MPa (c).

carbon atoms. When the pore structure is formed, one side of the coal surface molecule is in contact with the gas molecules, and the other side is attracted by carbon atoms. Under this unbalanced state, the surface molecules tend to move toward the interior of the coal.[40] The physical adsorption occurs when the coal surface produces van der Waals forces on the gas molecules. However, multilayer adsorption is analyzed from the organic structure of coal. In the low- and medium-metamorphism stage, the number of aromatic structures on the coal surface is rare and randomly distributed which is composed and supported by a large number of oxygen-containing functional groups, oxygen-containing bridges, and aliphatic side bonds.[41] As coalification enhanced, these side bond groups gradually fall off and become H_2O, CO_2, CO, CH_4, and so forth, resulting in an imbalance of the valence bond and force. Meanwhile, the specific surface energy is generated, and adsorption occurs finally. Moreover, for the multilayer, when adsorption reaches the dynamic equilibrium, the chemical potential is equal to each adjacent two layers in the equilibrium phase of the equilibrium equation; however, the adsorption heat of each layer is quite different.

2.2.3. Thermal Model. Adsorption heat is generated during the gas adsorption process, which reflects the energy change in the adsorption field on the coal surface. Under the isothermal condition, the gas adsorption on the coal surface is a process of reducing the surface free enthalpy and entropy; therefore, the specific surface energy can be measured by the calculation of the calorific value and further to determine the applicability of two different adsorption models.

During the adsorption−desorption process, the coal temperature is increased to different extents. The experiment is carried out in an incubator, and the ambient temperature affects the adsorption temperature. Therefore, the experiment was designed to analyze the stage of the sensitive change temperature. The temperature change is following the exponential function relationship, according to the curve of the temperature change with time, which is shown in eq 8[42]

$$\Delta T = \alpha(1 - e^{-t/\beta}) \tag{8}$$

where ΔT is the difference of the desorption temperature; α and β are fitting coefficients; and t is the adsorption time. The fitting coefficient (α) represents the temperature gap when time approaches infinity.

According to the thermodynamic formula, the heat generated by the gas adsorption process of the coal sample can be calculated,[43] which is shown in eq 9

$$\Delta E = cm\Delta T \tag{9}$$

where ΔE is the calorie change value; c is the specific heat capacity of coal, which is 1.46 (J/kg); m is the weight of the coal sample. The calorific value calculation results are shown in Table 5.

The change in the specific surface energy can be calculated based on the calorific value, as shown in Table 6.

The gas adsorption process is complicated, and the adsorption interaction of the coal surface is stronger than that between the adsorbate molecules. The comparison of the specific surface energy variation based on the single-layer adsorption model, multilayer model, and thermal model is shown in Figure 3.

It is clear that the trend of the specific surface energy variation based on the calorific value is closer to the multilayer adsorption calculation result. Only in the range of P/P_0 = 0.05−0.35, the BET multilayer adsorption equation is suitable, which is consistent with the experiment. Therefore, it is more reasonable to calculate the specific surface energy variation based on the multilayer adsorption model.

2.3. Microscopic Energy Simulation. *2.3.1. Functional Group Analysis.* The type and quantity of oxygen-containing functional groups of coal affect the gas adsorption capacity

https://dx.doi.org/10.1021/acsomega.0c00462
ACS Omega 2020, 5, 14976−14989

Table 5. Calorific Value of Coal Samples

	30 °C		40 °C		50 °C	
coal sample	ΔT (°C)	ΔE (J/g)	ΔT (°C)	ΔE (J/g)	ΔT (°C)	ΔE (J/g)
Kiamusze	0.86	377.83	0.67	295.23	0.52	228.31
	1.07	467.21	0.98	430.92	0.88	383.13
	1.49	650.96	1.39	607.32	1.13	492.82
	2.10	917.26	1.82	794.70	1.60	698.93
	3.17	1386.44	2.55	1117.47	2.35	1027.83
	3.33	1456.95	3.20	1400.01	2.98	1302.93
Panxi	0.78	381.30	0.63	306.70	0.63	305.87
	1.28	625.83	1.16	565.76	1.03	503.05
	1.95	951.19	1.90	923.42	1.82	884.54
	4.02	1956.61	3.96	1927.96	3.84	1868.67
	5.01	2439.44	4.90	2385.02	4.73	2305.46
	5.90	2872.24	5.64	2748.63	5.44	2648.27
Haitian	0.86	322.19	0.69	257.08	0.50	188.27
	1.02	383.69	0.79	294.13	0.69	259.74
	2.25	841.07	2.21	826.31	2.14	801.66
	3.26	1220.01	3.12	1170.19	3.06	1147.68
	3.59	1344.19	3.48	1302.76	3.40	1273.01
	4.14	1550.77	4.09	1532.64	3.83	1434.80
Pingba	0.39	181.01	0.22	103.79	0.20	94.73
	0.46	216.64	0.39	185.29	0.39	182.94
	1.06	496.14	0.92	433.52	0.88	412.87
	1.54	724.38	1.51	708.33	1.49	697.11
	1.95	914.69	1.91	895.12	1.84	864.98
	2.18	1021.16	2.18	1025.34	1.94	910.47
Pingbao	0.44	189.92	0.31	134.67	0.29	126.73
	0.61	265.54	0.58	254.86	0.50	219.14
	1.21	527.03	1.16	505.44	0.95	413.56
	1.88	821.62	1.76	768.80	1.53	667.45
	2.17	944.73	2.06	898.24	1.99	869.85
	2.67	1164.57	2.49	1085.59	2.18	950.09
Matigou	0.58	220.46	0.39	149.13	0.24	91.33
	0.92	348.92	0.84	317.58	0.73	276.30
	1.71	645.36	1.61	607.67	1.35	508.78
	2.32	875.35	2.04	769.50	1.82	686.79
	3.39	1280.55	2.77	1048.26	2.57	970.84
	3.55	1341.45	3.42	1292.27	3.20	1208.43
Ordos	0.76	334.35	0.57	251.60	0.42	184.54
	1.17	511.62	1.08	475.26	0.97	427.37
	1.91	838.60	1.81	794.88	1.55	680.15
	2.52	1105.42	2.24	982.63	2.02	886.67
	3.59	1575.51	2.98	1306.02	2.77	1216.20
	3.75	1646.16	3.62	1589.10	3.40	1491.83
Zhaozhuang	1.10	414.99	0.94	357.12	0.94	356.48
	1.60	604.72	1.48	558.11	1.35	509.46
	2.27	857.17	2.21	835.62	2.13	805.45
	4.33	1637.26	4.27	1615.03	4.15	1569.02
	5.32	2011.88	5.21	1969.65	5.05	1907.92
	6.21	2347.68	5.96	2251.77	5.75	2173.90

which can be analyzed using Fourier transform infrared (FTIR) spectroscopy.[44]

As shown in Figure 4, the types of functional groups contained in the eight coal samples are basically the same. The coal molecular skeleton has the aromatic core as the basic structural unit, and the aromatic rings are connected by different types of bridge bonds. The oxygen-containing functional groups, aliphatic hydrocarbons, and atomic groups are attached to the coal molecular skeleton. The main types of absorption peaks of the infrared spectrum are listed in Table 7.

The affinity analysis of spectral peaks based on the infrared spectra of eight coal samples displayed the absorption peak position and intensity which indicated the type and quantity of functional groups. To sum up, in the middle-rank bituminous coal samples (Pingba, Pingbao, and Haitian), the number of absorption peaks in the high wavenumber section is higher than that of other coal samples. Moreover, the Pingba and Haitian coal samples showed extremely low-intensity absorption peaks at low wavenumbers (1008.64, 1031.59 cm^{-1}). The gas adsorption capacity is mainly controlled by the adsorption energy.[45] As the content of oxygen-containing functional groups increases, the adsorption energy increases, and thus, the adsorption capacity is enhanced. For example, the Zhaozhuang coal sample contains more hydroxyl and carbonyl groups, which increase the ability of coal to adsorb gas. Therefore, unlike the single-layer adsorption model of physical adsorption, the existence of energy due to internal chemical changes makes the multilayer adsorption energy variation more accurately reflect the gas adsorption capacity. The specific surface energy variation has the same trend as the gas adsorption amount, which can be controlled by affecting the chemical reaction inside coal, thereby changing the adsorption capacity and finally improving the gas drainage effect.

2.3.2. Models. The oxygen-containing functional groups of coal are mainly composed of organic functional groups such as the carboxyl group, hydroxyl group, carbonyl group, and ether bond.[46] The basic structural unit of the molecular skeleton is an aromatic nucleus, and the oxygen-containing functional groups, aliphatic hydrocarbons, and atoms are connected by different bridge bonds. The structural unit of coal is shown in Figure 5.

We conducted simulations using Accelrys Materials Studio.[47] The coal structure unit model is shown in Figure 6.[48] The generalized gradient approximation (GGA) functional is used to replace the local gradient approximation functional, and the electron exchange−correlation potential is based on GGA-based PW91. We selected the DNP (dual-valued polarization basis set) module and unlimited the electron spin. Based on the convergence of the system energy and charge density distribution, the accuracy is higher than 10^{-5}, the energy convergence criterion is 2×10^{-5}, the force convergence criterion is 0.002, and the displacement convergence criterion is 0.005.

The adsorption energy of gas molecules at functional groups can be calculated using eq 10

$$E = E_{coal/gas} - E_{coal} - E_{gas} \quad (10)$$

where $E_{coal/gas}$ is the total energy after gas adsorption; E_{coal} is the total energy of coal; and E_{gas} is the total energy of gas.

According to the eq 10, the adsorption energy of gas molecules at different functional groups under the adsorption saturation condition are listed in Table 8.

The larger the absolute value of adsorption energy, the stronger is the adsorption capacity. Based on Table 8, the carboxyl group has the strongest adsorption energy, while the hydroxyl group is the opposite.

2.3.3. Quantitative Analysis of Functional Groups. The absorption spectrum of the infrared spectrum in coal is large, and the superposition peak can be processed to determine the functional group content.[49]

https://dx.doi.org/10.1021/acsomega.0c00462
ACS Omega 2020, 5, 14976−14989

Table 6. Specific Surface Energy Variation Calculated Using the Calorific Value

	change value (kJ/m^2)				change value (kJ/m^2)		
coal sample	30 °C	40 °C	50 °C	coal sample	30 °C	40 °C	50 °C
Kiamusze	1313.31	1026.20	793.63	Panxi	1049.50	844.21	841.90
	1623.92	1497.81	1331.70		1722.62	1557.33	1384.67
	2262.61	2110.92	1712.94		2618.25	2541.83	2434.68
	3188.31	2762.34	2429.42		5385.69	5306.82	5143.59
	4819.00	3884.10	3572.65		6714.70	6564.94	6345.88
	5064.11	4866.22	4528.77		7906.00	7565.70	7289.43
Haitian	1538.17	1227.42	898.79	Pingba	908.31	520.80	475.22
	1831.77	1404.25	1240.10		1087.13	929.72	918.00
	4015.36	3945.00	3827.32		2489.64	2175.29	2071.68
	5824.49	5586.69	5479.23		3634.79	3554.22	3498.00
	6417.37	6219.62	6077.63		4589.77	4491.34	4340.32
	7403.68	7317.11	6850.00		5124.00	5145.00	4568.65
Pingbao	1084.48	769.00	723.71	Matigou	778.52	526.60	322.49
	1516.27	1455.33	1251.44		1232.00	1121.42	975.56
	3009.49	2886.34	2361.64		2278.82	2145.72	1796.50
	4691.67	4390.20	3811.38		3090.94	2717.21	2425.12
	5394.72	5129.30	4967.20		4521.71	3701.47	3428.13
	6650.11	6199.15	5425.41		4736.84	4563.10	4267.00
Ordos	989.20	744.38	546.00	Zhaozhuang	1114.74	959.23	957.54
	1513.74	1406.10	1264.44		1624.32	1499.10	1368.40
	2481.09	2351.68	2012.36		2302.38	2244.44	2163.49
	3270.47	2907.21	2623.32		4397.70	4338.00	4214.38
	4661.27	3864.00	3598.20		5403.90	5290.53	5124.66
	4870.28	4701.52	4413.70		6305.92	6048.30	5839.12

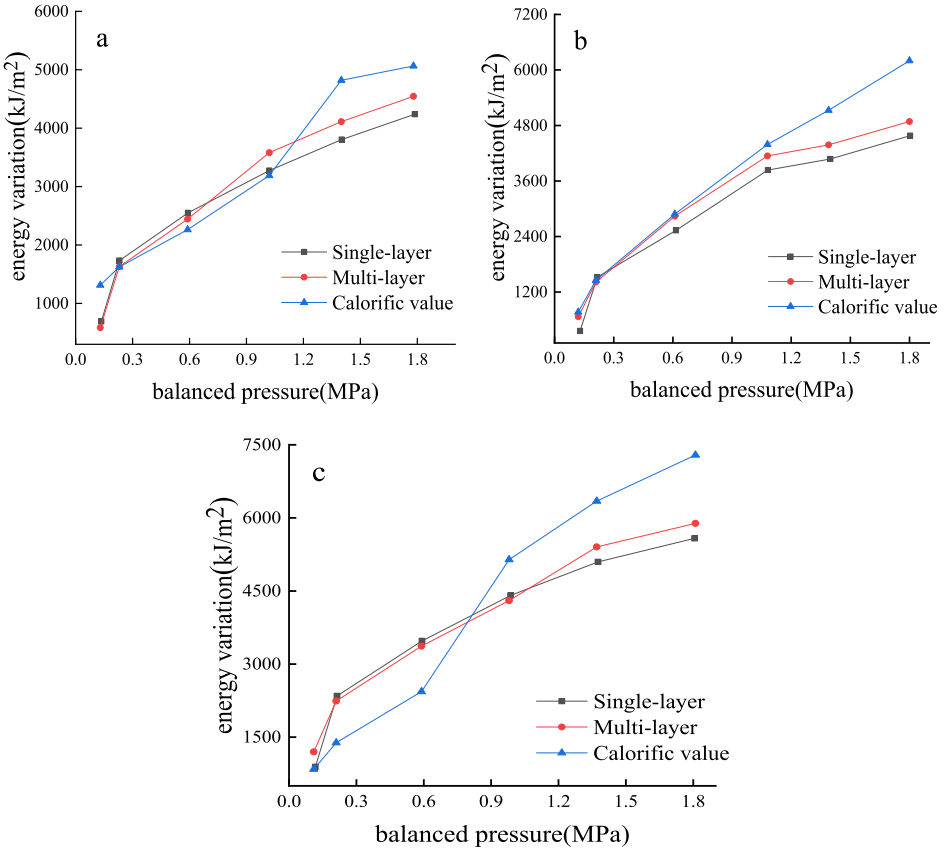

Figure 3. Energy variation calculated based on the single-layer model (black), multilayer model (red), and calorific value (blue). Kiamuse at 30 °C (a); Pingbao at 40 °C (b); Panxi at 50 °C (c).

https://dx.doi.org/10.1021/acsomega.0c00462
ACS Omega 2020, 5, 14976−14989

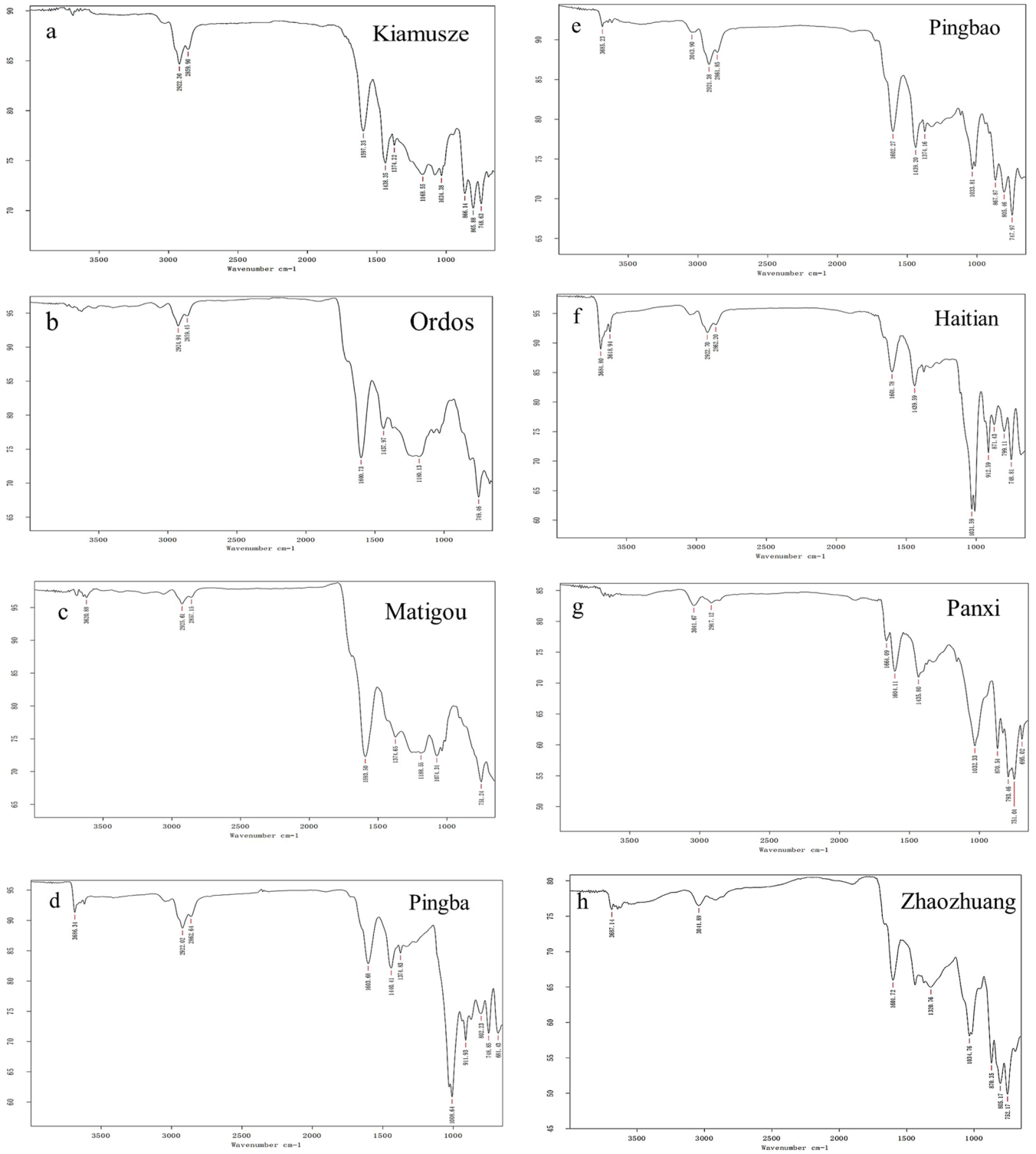

Figure 4. Infrared spectrogram of coal samples. Kiamuse (a); Ordos (b); Matigou (c); Pingba (d); Pingbao (e); Haitian (f); Panxi (g); Zhaozhuang (h).

Table 7. Wavelength Corresponding to the Absorption Peak

absorption peak	wavelength (cm^{-1})
aliphatic structure	1380, 1460, 2800−3000
aromatic structure	750, 800, 850, 1500
oxygen-containing functional group	1200−900, 1650, 3460
benzene ring	700−900

The relationship between the content of hydroxyl (C_{OH}) in coal and the adsorption capacity (A) can be expressed as follows

$$A = 9.0791C_{OH} + 16.548 \quad (11)$$

The relationship between the content of carboxyl (C_{COOH}) in coal and the adsorption capacity (A) can be expressed as follows

https://dx.doi.org/10.1021/acsomega.0c00462
ACS Omega 2020, 5, 14976−14989

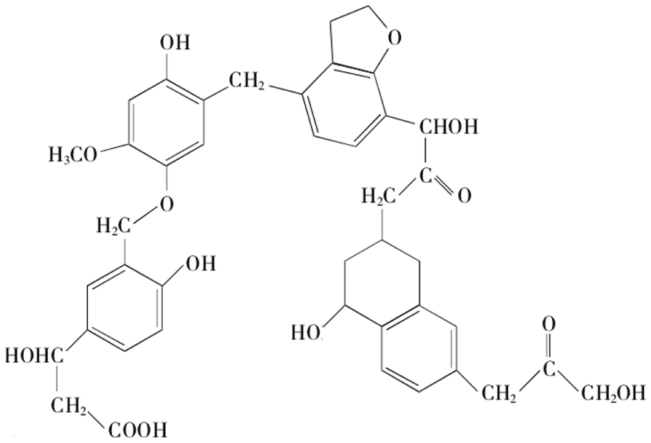

Figure 5. Coal structural unit model.

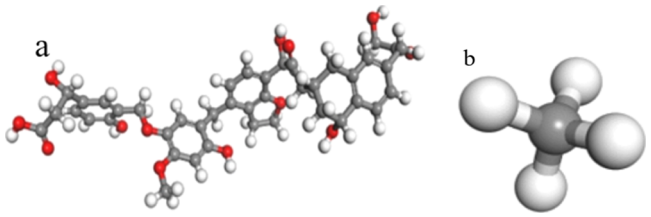

Figure 6. Molecular model of coal (a) and methane (b).

$$A = 2.67C_{COOH} + 5.08 \quad (12)$$

The relationship between the content of other oxygen-containing functional groups (C_{other}) in coal and the adsorption capacity (A) can be expressed as follows

$$A = 8.47C_{other} + 33.84 \quad (13)$$

with eqs 11 and 13, the coal functional group content can be calculated based on FTIR spectroscopy, which is shown in Table 9.

Unlike the type of functional group, according to Table 9, the functional group content of coal samples is changing as the coal rank increases, which is one of the reasons for the energy difference of coal samples.

2.3.4. Adsorption Energy Calculation and Comparative Analysis. Each coal sample weighs 300 g, and the functional group content in the coal sample can be quantitatively estimated according to Table 9. Therefore, with Table 8, the total adsorption energy of each coal sample is listed in Table 10.

As shown in Table 10, the total adsorption energy is different because of the functional group content of coal samples. According to the microscopic calculation, the adsorption energy relationship between the eight coal samples is Zhaozhuang > Panxi > Ordos > Haitian > Matigou > Pingbao > Pingba > Kiamusze, which is consistent with the law of the surface free energy amount.

The adsorption energy calculated based on the functional groups is close to the surface free energy based on the multilayer adsorption model; however, there are still certain differences. The possible causes are as follows: (i) the experimental coal samples are impure, resulting in energy differences. (ii) The calculation of the adsorption energy of the functional group is based on the coal-saturated adsorption methane simulation, while the experimental adsorption only for 12 h is not long enough, and thus, the adsorption may be incomplete. (iii) The calculation of surface free energy variation belongs to the macroscopic analysis; in contrast, the calculation of functional group adsorption energy belongs to microscopic analysis, and there is a scale effect between them, which leads to the energy difference. The comparison is displayed in Figure 7.

Table 9. Functional Mass Content of Coal

	content (mol/kg)				
coal sample	hydroxy	carboxy	carbonyl	ether bond	methyl
Kiamusze	8.64	32.93	6.28	6.51	6.04
Panxi	8.81	29.93	5.45	5.80	5.33
Haitian	7.43	28.06	5.10	5.27	4.74
Pingba	8.75	29.93	4.98	5.45	5.45
Pingbao	6.66	26.19	4.27	4.51	3.80
Ordos	8.31	29.93	5.45	5.69	5.33
Matigou	7.98	28.81	5.57	5.80	4.98
Zhaozhuang	8.53	31.43	6.16	6.34	5.80

Table 10. Functional Group Adsorption Energy

	adsorption energy (kJ/m^2)				
coal sample	0.2	0.6	1.0	1.4	1.8
Kiamusze	3158.61	3505.10	4985.12	5136.43	5310.91
Panxi	3430.22	3914.82	5439.44	5604.27	5797.00
Haitian	3419.30	3776.49	5284.42	5444.33	5631.33
Pingba	2888.10	2449.48	3819.42	3934.88	4072.92
Pingbao	2330.14	3061.27	4493.77	4628.73	4789.88
Ordos	3339.42	3727.30	5230.90	5389.16	5574.31
Matigou	3275.91	3611.61	5102.41	5257.75	5436.47
Zhaozhuang	3849.23	4426.12	6003.54	6186.00	6395.41

2.4. Discussion on the Mechanism of Gas Adsorption. Energy variation is affected by chemical bonds, which is the intermolecular force. The main cause of gas adsorption to methane is van der Waals force, which includes dispersive force, orientation force, and induction force.[14] The van der Waals force generally refers to the sum of weak interactions in addition to strong interaction forces such as covalent bonds and Coulomb forces. As the distance decreases, the intermolecular force becomes larger. In addition, the

Table 8. Adsorption Energy of the Gas Molecule on Different Functional Groups

	adsorption energy at functional groups (kJ/mol)				
adsorption position	0.2 MPa	0.6 MPa	1.0 MPa	1.4 MPa	1.8 MPa
hydroxy	−9.0336	−8.8062	−9.23487	−9.44276	−10.0356
carboxy	−30.2286	−35.8874	−40.0358	−41.1809	−42.9653
carbonyl	−28.7463	−30.2324	−33.2486	−34.8858	−34.9887
ether bond	−26.0203	−26.6606	−29.0589	−30.1644	−30.1759
methyl	−20.688	−22.2985	−24.3226	−24.6561	−25.2207

https://dx.doi.org/10.1021/acsomega.0c00462
ACS Omega 2020, 5, 14976−14989

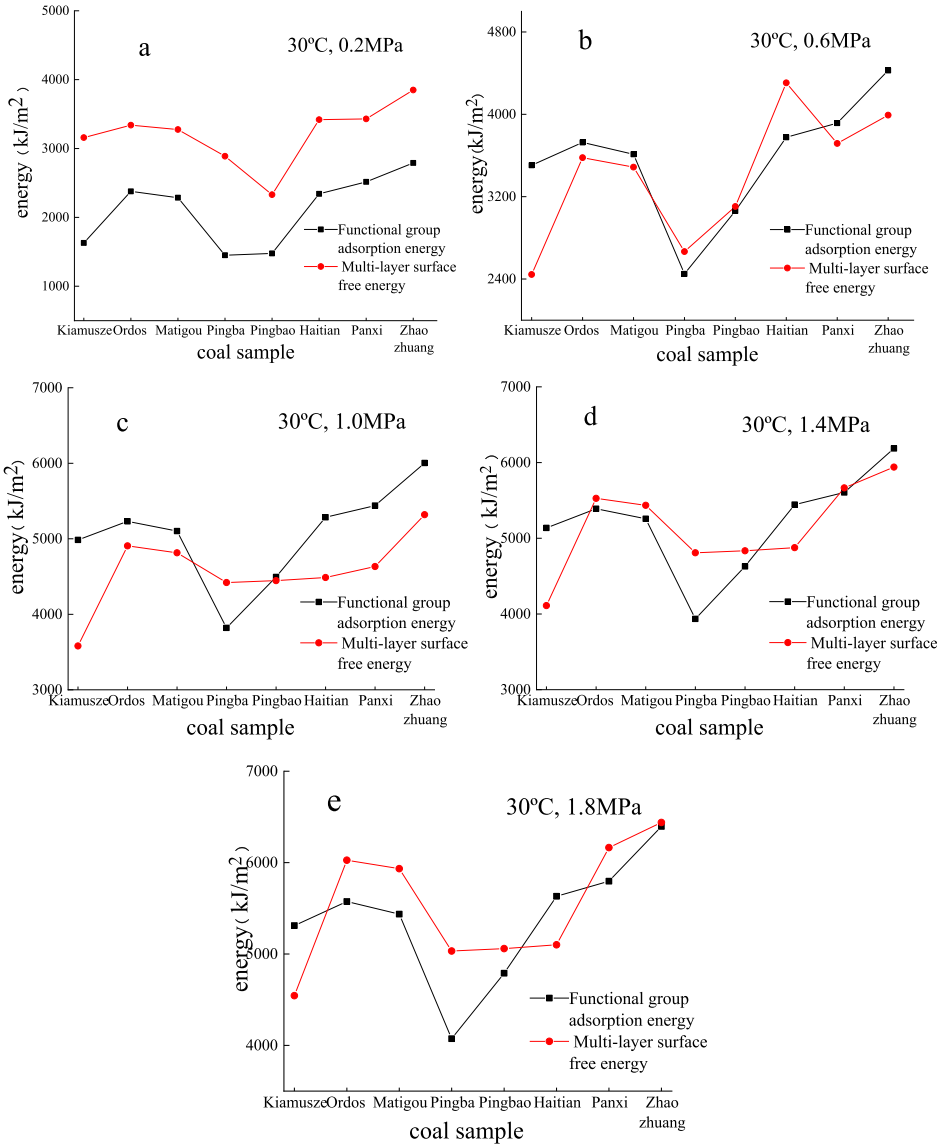

Figure 7. Energy calculated using the functional group (black) and multilayer model (red) at 30 °C under 0.2 (a), 0.6 (b), 1.0 (c), 1.4 (d), and 1.8 MPa (e).

adsorption capacity of each atom on the coal macromolecules surface is different, and the strong ability will form adsorption vacancies, thereby adsorbing methane molecules. In the long process of coalification, as the degree of coalification increases, the number of rings forming the skeleton structure increases. In the meantime, the number of side chains and heteroatom-containing functional groups connected the skeleton structure to become shorter. Therefore, the carbon content increases continuously, and the specific surface area and electrostatic force increases, which leads to an increase in the adsorption capacity.[43] As shown in Table 1, the Zhaozhuang coal sample has the largest specific surface area of 149.41 m^2/g; therefore, the electrostatic force of the Zhaozhuang sample is relatively large, which means the largest energy variation and the strongest adsorption capacity. It is clear that the higher the surface energy, the easier the coal sample adsorbs gas, and thus, the more difficult it is for gas to migrate in such coal seams, which means it is more difficult to conduct gas drainage on such coal seams.

In general, the change of adsorption energy affects the adsorption capacity, and the energy variation is also affected by the microstructure of the coal samples and internal chemical structure. Therefore, it is possible to explore how to affect gas desorption and achieve the purpose of improving the gas drainage effect from the perspective of changing energy.

3. CONCLUSIONS

In this work, the specific surface energy of eight different rank coal samples was investigated through a macro- and micro-scale. Two different adsorption models and a thermal model were used to calculate the specific surface energy based on the adsorption−desorption experiment. Moreover, the impact of types and quantities of functional groups in different coal samples were discussed in detail using infrared chromatography and molecular simulation. The main conclusions are summarized as follows:

- We have established the computation equations of adsorption energy based on the BET model and Langmuir model and verified them with a thermal

https://dx.doi.org/10.1021/acsomega.0c00462
ACS Omega 2020, 5, 14976−14989

Table 11. Collection Site for Coal Samples

coal sample	working face	coal mine	province	region
Kiamusze	41112	Zhenxing coal mine of the Hegang Mining Group	Heilongjiang	Northeast of China
Ordos	311101	Ordos coal mine of the Shenhua Mining Group	Inner Mongolia	North China
Matigou	25111	Matigou coal mine of the Huating Mining Group	Gansu	Northwest of China
Pingba	12112	Pingdingshan no. 8 coal mine of the Pingdingshan Mining Group	Henan	Central China
Pingbao	12010	Shoushan no. 1 coal mine of the Henan Pingbao Mining Group	Henan	Central China
Haitian	3616	Haitian coal mine of the Jinmei Mining Group	Shanxi	Central China
Panxi	6196	Panxi coal mine of the Xinwen Mining Group	Shandong	Central China
Zhaozhuang	3305	Zhaozhuang coal mine of the Jinmei Mining Group	Shanxi	Central China

model. The result demonstrated that the energy value obtained using the BET model is closer to the actual energy variation.

- The specific surface energy variation calculated based on the BET model can be used to measure the gas adsorption capacity. Moreover, the relationship between adsorption capacity of different rank coal samples is as follows: the high-rank bituminous and anthracite coal > low-rank bituminous coal > middle-rank bituminous coal. The result can provide a new view for evaluating CBM storage and migration in the coal seam.
- The macromolecular structure of coal determines the gas adsorption in a form that affects the adsorption energy. During different coalification stages, the types of functional groups are the same; however, the functional group content is unequal. Among the five types of functional groups, the adsorption energy of the carboxyl group is the largest, while the adsorption energy of the hydroxyl group is the least.

4. SAMPLES AND METHOD

4.1. Samples. The samples analyzed in this study are obtained from China. The specific locations for collecting coal samples are listed in Table 11.

According to the GB/T 212-2008, the quantitative analyses of the coal composition and coal rank of the samples were obtained using the industrial analyzer. The proximate analysis of the eight coals used in this paper is summarized in Table 12.

4.2. Experimental Methods.

(i) The experimental system is mainly used to determine the pressure and temperature variation of the coal sample during the adsorption−desorption process which contains four subsystems. (a) Gas control system: the test gases are nitrogen, helium, and methane, and the pressure inside the cylinder is 10 MPa; (b) adsorption−desorption system: including the thermostatic box, sample tank, and reference tank; (c) pressure sensing system: including data acquisition module and pressure sensor. (d) Temperature measurement system: platinum resistance temperature sensor and temperature acquisition module. The experimental schematic is shown in Figure 8.

Table 12. Industrial Analysis of Coal Samples

coal sample	coal rank	moisture (%)	ash (%)	volatile (%)	fixed carbon (%)
Kiamusze	low-rank bituminous coal	0.81	14.90	28.05	56.59
Ordos	low-rank bituminous coal	4.77	3.30	32.24	60.81
Matigou	middle-rank bituminous coal	9.54	8.37	25.38	58.12
Pingba	middle-rank bituminous coal	0.67	16.11	20.39	62.88
Pingbao	middle-rank bituminous coal	0.66	8.21	18.47	72.74
Haitian	high-rank bituminous coal	0.66	14.24	11.73	73.54
Panxi	high-rank bituminous coal	1.83	16.61	11.29	70.78
Zhaozhuang	anthracite	1.51	28.36	7.70	62.98

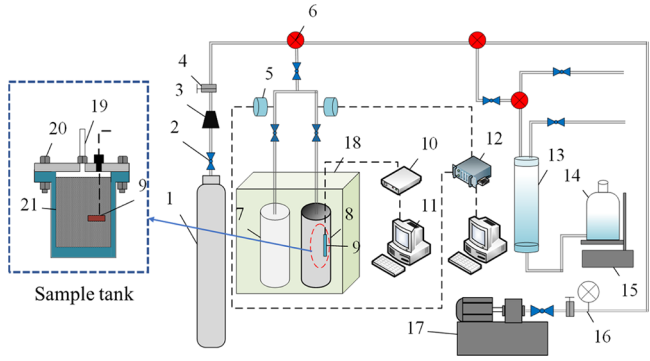

Figure 8. Adsorption−desorption experimental device. (1) High-pressure gas tank; (2) switch valve; (3) pressure-reducing valve; (4) pressure-adjusting valve; (5) pressure sensor; (6) three-way valve; (7) reference tank; (8) sample tank; (9) temperature sensor; (10) temperature-measuring meter; (11) computer; (12) pressure acquisition device; (13) graduated cylinder; (14) water bottle; (15) platform; (16) pressure gauge; (17) vacuum pump; (18) incubator; (19) air outlet; (20) bolt; and (21) coal sample.

(ii) Eight kinds of 300 g of coal samples were subjected to gas adsorption experiments for 12 h and gas desorption experiments for about 6 h. The temperature of the incubator was set at 30, 40, and 50 °C, and the gas adsorption pressure were 0.1, 0.2, 0.6, 1.0, 1.4, and 1.8 MPa. Finally, the adsorption capacity, adsorption rate, desorption amount, desorption rate, and corresponding temperature changes in the adsorption and adsorption−desorption processes of each coal sample were obtained.

APPENDIX A

Equation Development

Single-Layer Adsorption. According to the Langmuir adsorption equation[50,51]

$$V = \frac{abP}{1 + bP} \tag{14}$$

https://dx.doi.org/10.1021/acsomega.0c00462
ACS Omega 2020, 5, 14976−14989

where a is the saturated adsorption capacity; b is the adsorption equilibrium constant; P is the gas pressure; V is the adsorption amount.

With eqs 3 and 14, the difference in surface tension can be rewritten as follows

$$\Delta\sigma = \frac{RT}{V_0 S}\int_0^P \frac{abP}{1+bP}\,\mathrm{d}P = \frac{aRT}{V_0 S}\ln(1+bP) \tag{15}$$

where σ is the surface tension; R is the universal gas constant; T is the absolute temperature; V_0 is the molar volume; S is the specific surface area of coal.

According to eq 15, the surface tension of coal depends on the amount of adsorption, the surface structure, the temperature of the adsorption system, and the pressure of the gas.

Differentiating P in eq 15, the specific surface energy variation at each pressure point can be defined as

$$\Delta\sigma_{P_1} = \frac{abRT}{V_0 S(1+bP)} \tag{16}$$

Multilayer Adsorption. Assume that gas adsorption is consistent with multimolecular layer adsorption, based on the BET equation, and the following can be written as[52,53]

$$\frac{P}{V(P_0-P)} = \frac{1}{V_m C} + \frac{C-1}{V_m C}\cdot\frac{P}{P_0} \tag{17}$$

where V_m is the multilayer saturated adsorption capacity of coal; C is the constant related to sample adsorption capacity; P is the adsorption pressure; V is the actual adsorption amount of the coal sample.

With eqs 3 and 17, the following equation can be written as

$$\Delta\sigma = \frac{RT}{V_0 S}\int_0^P \frac{CV_m}{[1+(C-1)(P/P_0)](P_0-P)}\,\mathrm{d}P = -\frac{RTV_m}{V_0 S}\ln\left|\frac{P-P_0}{P-P_0-CP}\right| \tag{18}$$

Differentiating P in eq 18, the specific surface energy variation can be defined as

$$\Delta\sigma_{P_2} = -\frac{RTV_m}{V_0 S(P-P_0)}\cdot\frac{CP_0}{(P-P_0)(P-P_0-CP)} \tag{19}$$

AUTHOR INFORMATION

Corresponding Authors

Xiangchun Li − *School of Emergency Management and Safety Engineering, China University of Mining & Technology, Beijing 100089, China; State Key Laboratory of Coal Resources and Safe Mining, Beijing 100083, China; State Key Laboratory of Cultivation Base for Gas Geology and Gas Control, Jiaozuo 454000, China*; Email: chinalixc123@163.com

Xiaolong Chen − *School of Emergency Management and Safety Engineering, China University of Mining & Technology, Beijing 100089, China*; orcid.org/0000-0003-3457-1357; Email: 18155843163@163.com

Authors

Fan Zhang − *School of Emergency Management and Safety Engineering, China University of Mining & Technology, Beijing 100089, China*

Mengting Zhang − *School of Emergency Management and Safety Engineering, China University of Mining & Technology, Beijing 100089, China*

Qi Zhang − *School of Emergency Management and Safety Engineering, China University of Mining & Technology, Beijing 100089, China*; orcid.org/0000-0002-5685-6823

Suye Jia − *School of Emergency Management and Safety Engineering, China University of Mining & Technology, Beijing 100089, China*

Complete contact information is available at: https://pubs.acs.org/10.1021/acsomega.0c00462

Notes

The authors declare no competing financial interest.

ACKNOWLEDGMENTS

This work was financially supported by the Natural Science Foundation of Beijing Municipality (grant no. 8192036), the National Key Research and Development Program of China (grant no. 2018YFC0808301), the Youth Foundation of Social Science and Humanity, the Ministry of Education of China (grant no. 19YJCZH087), the State Key Laboratory Cultivation Base for Gas Geology and Gas Control (Henan Polytechnic University) (grant no. WS2018B04), and the Fundamental Research Foundation for the Central Universities (grant no. 2009QZ09).

REFERENCES

(1) Wu, Y.; Gao, R.; Yang, J. Prediction of coal and gas outburst: A method based on the BP neural network optimized by GASA. *Process Saf. Environ. Prot.* **2020**, *133*, 64−72.

(2) Fu, G.; Xie, X.; Jia, Q.; Tong, W.; Ge, Y. Accidents analysis and prevention of coal and gas outburst: Understanding human errors in accidents. *Process Saf. Environ. Prot.* **2020**, *134*, 1−23.

(3) Dong, J.; Cheng, Y.; Jin, K.; Zhang, H.; Liu, Q.; Jiang, J.; Hu, B. Effects of diffusion and suction negative pressure on coalbed methane extraction and a new measure to increase the methane utilization rate. *Fuel* **2017**, *197*, 70−81.

(4) Cai, Y.; Liu, D.; Pan, Z.; Yao, Y.; Li, J.; Qiu, Y. Pore structure and its impact on CH_4 adsorption capacity and flow capability of bituminous and subbituminous coals from Northeast China. *Fuel* **2013**, *103*, 258−268.

(5) Li, Z.; Liu, D.; Cai, Y.; Wang, Y.; Teng, J. Adsorption pore structure and its fractal characteristics of coals by N_2 adsorption/desorption and FESEM image analyses. *Fuel* **2019**, *257*, 116031.

(6) Cui, Y. J.; Zhang, Q. L.; Yang, X. Adsorption performance of different coals and the variation law of equal adsorption heat. *Nat. Gas Ind.* **2003**, *23*, 130−131.

(7) Pan, J.; Wang, K.; Hou, Q.; Niu, Q.; Wang, H.; Ji, Z. Micro-pores and fractures of coals analyzed by field emission scanning electron microscopy and fractal theory. *Fuel* **2016**, *164*, 277−285.

(8) Ariunaa, A.; Liou, S. Y.-H.; Tsatsral, G.; Purevsuren, B.; Davaajav, Y.; Chang, R.-W.; Lin, C.-J. Selective adsorption of greenhouse gases on the residual carbon in lignite coal liquefaction. *J. Taiwan Inst. Chem. Eng.* **2018**, *85*, 170−175.

(9) He, M. C.; Wang, C. G.; Li, D. J.; Liu, J.; Zhang, X. H. Desorption characteristic of adsorbed gas in coal samples under coupling temperature and uniaxial compression. *Chin. J. Rock Mech. Eng.* **2010**, *29*, 865−872.

(10) Yang, R. T.; Saunders, J. T. Adsorption of gases on coals and heattreated coals at elevated temperature and pressure: Adsorption from hydrogen and methane as single gases. *Fuel* **1985**, *64*, 616−620.

(11) Tang, X.; Ripepi, N. High pressure supercritical carbon dioxide adsorption in coal: Adsorption model and thermodynamic characteristics. *J. CO_2 Util.* **2017**, *18*, 189−197.

(12) Hao, S.; Chu, W.; Jiang, Q.; Yu, X. Methane adsorption characteristics on coal surface above critical temperature through Dubinin−Astakhov model and Langmuir model. *Colloids Surf., A* **2014**, *444*, 104−113.

(13) Li, Y.; Zhang, C.; Tang, D.; Gan, Q.; Niu, X.; Wang, K.; Shen, R. Coal pore size distributions controlled by the coalification process: An experimental study of coals from the Junggar, Ordos and Qinshui basins in China. *Fuel* **2017**, *206*, 352−363.
(14) Xiao, J.; Li, F.; Zhong, Q.; Huang, J.; Wang, B.; Zhang, Y. Effect of high-temperature pyrolysis on the structure and properties of coal and petroleum coke. *J. Anal. Appl. Pyrolysis* **2016**, *117*, 64−71.
(15) Li, W.; Cheng, Y.; Wu, D.; An, F. CO_2 Isothermal Adsorption Models of Coal in the Haishiwan Coalfield. *Min. Sci. Technol.* **2010**, *20*, 281−285.
(16) Meng, Z. P.; Tian, Y. D.; Li, G. F. Basic physical properties of coal. In *Theory and Method of Coalbed Methane Development Geology*, 2nd ed.; Sun, K. W., Ed.; Science Press: Beijing, 2010; pp 23−29.
(17) Chen, Z. H.; Wang, Y. B.; Song, Y. Comparison of adsorption/desorption properties of CBM in different rank coals. *Nat. Gas Ind.* **2008**, *3*, 30−32.
(18) Stamboliadis, E. T. The energy distribution theory of comminution specific surface energy, mill efficiency and distribution mode. *Miner. Eng.* **2007**, *20*, 140−145.
(19) Zhou, L.; Feng, Q.-Y.; Qin, Y. Thermodynamic analysis of competitive adsorption of CO_2 and CH_4 on coal matrix. *J. China Coal Soc.* **2011**, *36*, 1307−1311.
(20) Holysz, L. Surface free energy and floatability of low-rank coal. *Fuel* **1996**, *75*, 737−742.
(21) Jańczuk, B.; Wójcik, W.; Zdziennicka, A.; Bruque, J. M. Components of the surface free energy of low rank coals in the presence of n-alkanes. *Powder Technol.* **1996**, *86*, 229−238.
(22) Burdzik, A.; Stähler, M.; Carmo, M.; Stolten, D. Impact of reference values used for surface free energy determination: An uncertainty analysis. *Int. J. Adhes. Adhes.* **2018**, *82*, 1−7.
(23) Zhang, L.; Aziz, N.; Ren, T. X.; Wang, Z. Influence of temperature on coal sorption characteristics and the theory of coal surface free energy. *Procedia Eng.* **2011**, *26*, 1430−1439.
(24) Jiménez, F.; Mondragón, F.; López, D. High-pressure thermogravimetric adsorption of CO2 for BET surface area calculations. *J. Therm. Anal. Calorim.* **2015**, *120*, 1723−1730.
(25) Zhou, S.; Zhang, D.; Wang, H.; Li, X. A modified BET equation to investigate supercritical methane adsorption mechanisms in shale. *Mar. Pet. Geol.* **2019**, *105*, 284−292.
(26) Pillalamarry, M.; Harpalani, S.; Liu, S. Gas diffusion behavior of coal and its impact on production from coalbed methane reservoirs. *Int. J. Coal Geol.* **2011**, *86*, 342−348.
(27) Crosdale, P. J.; Moore, T. A.; Mares, T. E. Influence of moisture content and temperature on methane adsorption isotherm analysis for coals from a low-rank, biogenically-sourced gas reservoir. *Int. J. Coal Geol.* **2008**, *76*, 166−174.
(28) Sakurovs, R.; Day, S.; Weir, S.; Duffy, G. Temperature dependence of sorption of gases by coals and charcoals. *Int. J. Coal Geol.* **2008**, *73*, 250−258.
(29) Xie, K. C. Microstructure of coal. In *Coal Structure and Reactivity*, 1st ed.; Liu, J. L., Ed.; Science Press: Beijing, 2002; pp 68−72.
(30) Nie, B.; He, X.; Wang, E. Surface Free Energy of Coal and Its Calculation. *J. Taiyuan Univ. Technol.* **2000**, *31*, 346−348.
(31) Zhang, W.; Kassab, G. S. Remodeling of conduit arteries in hypertension and flow-overload obeys a minimum energy principle. *J. Biomech.* **2008**, *41*, 2567−2570.
(32) Guo, P.; Cao, S. G.; Zhang, Z. G. Theoretical study of deformation model of coal swelling induced by gas adsorption. *Rock Soil Mech.* **2014**, *35*, 3467−3472.
(33) Chen, X. Z.; Cai, Z. Y. Thermodynamic calculation of heterogeneous systems. In *Chemical Thermodynamics*, 1st ed.; Luo, W. M., Ed.; Chemical Industry Press: Beijing, 2004; pp 163−170.
(34) Gu, T. R.; Zhu, B. Y.; Li, W. L. Solid surface. In *Interface Chemistry*, 1st ed.; Liu, J. L., Ed.; Science Press: Beijing, 1994; pp 191−216.
(35) McClellan, A. L.; Harnsberger, H. F. Cross-sectional areas of molecules adsorbed on solid surfaces. *J. Colloid Interface Sci.* **1967**, *23*, 577−599.
(36) Wang, G.; Wang, K.; Ren, T. Improved analytic methods for coal surface area and pore size distribution determination using 77K nitrogen adsorption experiment. *Int. J. Min. Sci. Technol.* **2014**, *24*, 329−334.
(37) Crosdale, P. J.; Beamish, B. B.; Valix, M. Coal bed methane sorption related to coal composition. *Int. J. Coal Geol.* **1998**, *35*, 147−158.
(38) Laxminarayana, C.; Crosdale, P. Controls on methane sorption capacity of Indian coals. *AAPG Bull.* **2002**, *86*, 201−212.
(39) Mastalerz, M.; Gluskoter, H.; Rupp, J. Carbon dioxide and methane sorption in high volatile bituminous coals from Indiana, USA. *Int. J. Coal Geol.* **2004**, *60*, 43−55.
(40) Wu, J. Coal adsorption method of calculating-coal surface energy and it's significance. *Coal Geol. Explor.* **1994**, *22*, 18−23.
(41) Yang, Q. Adsorption of real gases in multimolecular layers. *Chin. J. Chem. Phys.* **1991**, *6*, 458−463.
(42) Zhang, T.-J.; Xu, H.-J.; Li, S.-G.; Ren, S.-X. The effect of temperature on the adsorbing capability of coal. *J. China Coal Soc.* **2009**, *34*, 802−805.
(43) Fu, Y. First law. In *Introduction to Chemical Thermodynamics*, 3rd ed.; Sun, K. W., Ed.; Science Press: Beijing, 2010; pp 21−29.
(44) Chen, Y.; Mastalerz, M.; Schimmelmann, A. Characterization of chemical functional groups in macerals across different coal ranks via micro-FTIR spectroscopy. *Int. J. Coal Geol.* **2012**, *104*, 22.
(45) Zhou, F.; Liu, S.; Pang, Y.; Li, J.; Xin, H. Effects of coal functional groups on adsorption microheat of coal bed methane. *Energy Fuels* **2015**, *29*, 1550−1557.
(46) Cui, Q.; Yang, M.; Zhang, X. X.; Gao, H.; Wang, G. Introduction to the analysis methods of oxygen functional groups in Coal. *Chem. Bull.* **2012**, *75*, 808−814.
(47) Meng, Z.; Li, X.; Lv, F.; Zhang, Q.; Chu, P. K.; Zhang, Y. Structure, molecular simulation, and release of a spirin from intercalated Zn−Al-layered double hydroxides. *Colloids Surf., B* **2015**, *135*, 339−345.
(48) Meng, J.; Zhong, R.; Li, S.; Yin, F.; Nie, B. Molecular model construction and study on gas adsorption of Zhaozhuang coal. *Energy Fuels* **2018**, *32*, 9727−9737.
(49) Zhu, X.; Zhu, Z.; Zhang, C. Quantitative analysis of oxygen functional groups in coal by infrared spectroscopy. *J. Fuel Chem. Technol.* **1999**, *27*, 335−339.
(50) Langmuir, I. The constitution and fundamental properties of solids and liquids. *J. Am. Chem. Soc.* **1916**, *38*, 2221.
(51) Dreisbach, F.; Staudt, R.; Keller, J. U. High Pressure Adsorption Data of Methane, Nitrogen, Carbon Dioxide and their Binary and Ternary Mixtures on Activated Carbon. *Adsorption* **1999**, *5*, 215−227.
(52) Brunauer, S.; Emmett, P. H.; Teller, E. Adsorption of gases in multimolecular layers. *J. Am. Chem. Soc.* **1938**, *60*, 309−319.
(53) Aranovich, G. L.; Donohue, M. D. A new approach to analysis of multilayer adsorption. *J. Colloid Interface Sci.* **1995**, *173*, 515−520.

https://dx.doi.org/10.1021/acsomega.0c00462
ACS Omega 2020, 5, 14976−14989